The Inception of Star Cluster Formation Revealed by [CII] Emission Around an Infrared Dark Cloud

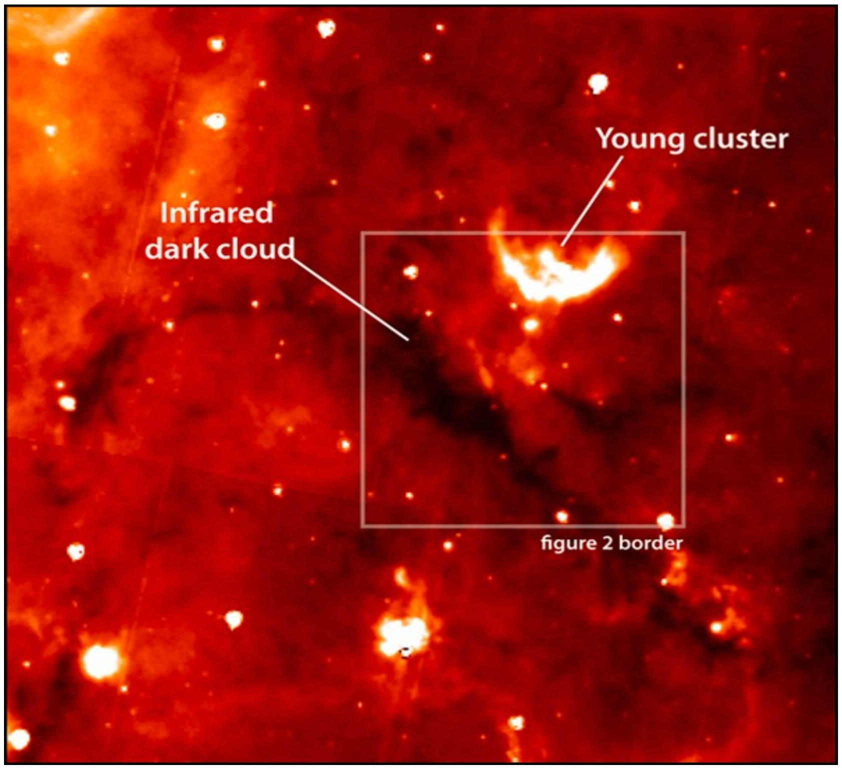

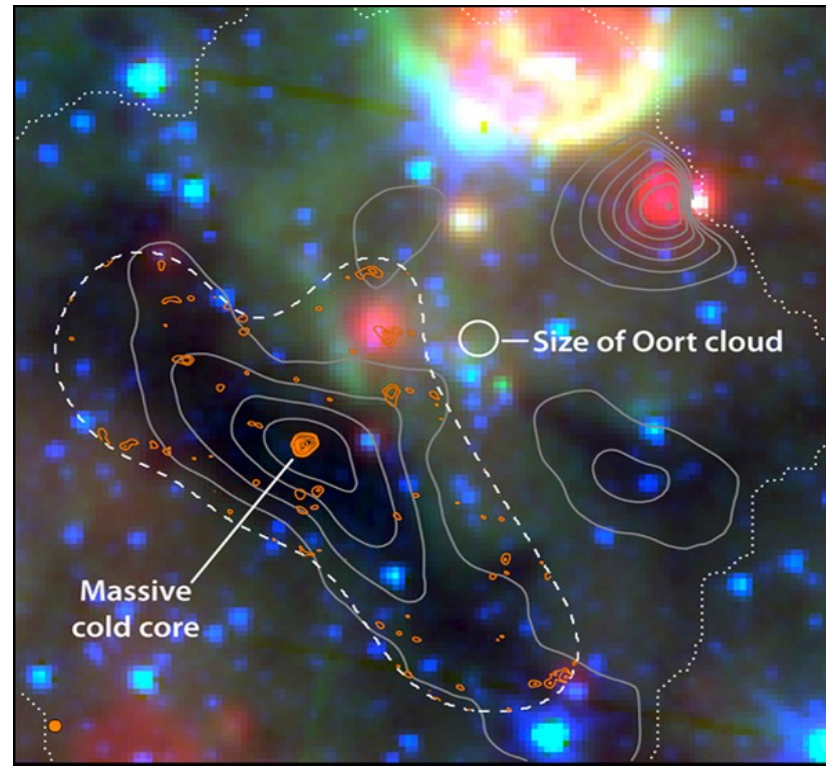

Thomas G. Bisbas
tbisbas@gmail.com

University of Virginia

5/23/18

Outline of the presentation

1. Introduction

2. Maghetohydrodynamical simulations of cloud-cloud collisions

3. Synthetic observations and new diagnostics of cloud-cloud collisions

4. SOFIA-upGREAT [CII] 158um observations of IRDC G35

GMC-GMC collisions

Giant Molecular Cloud (GMC) collisions are a potential mechanism for triggering star formation activity in such clouds.

GMC collisions may even set global star formation rates (SFRs) of disk galaxies

It is an attractive mechanism because it is a process that is expected to create ~parsec-scale dense gas clumps that are prone to gravitational instability and are the precursors to star clusters, while at the same time being sensitive to global galactic dynamics, such as shear rate (e.g. Tan 2000, 2010) and the presence of spiral arms (Dobbs 2008)

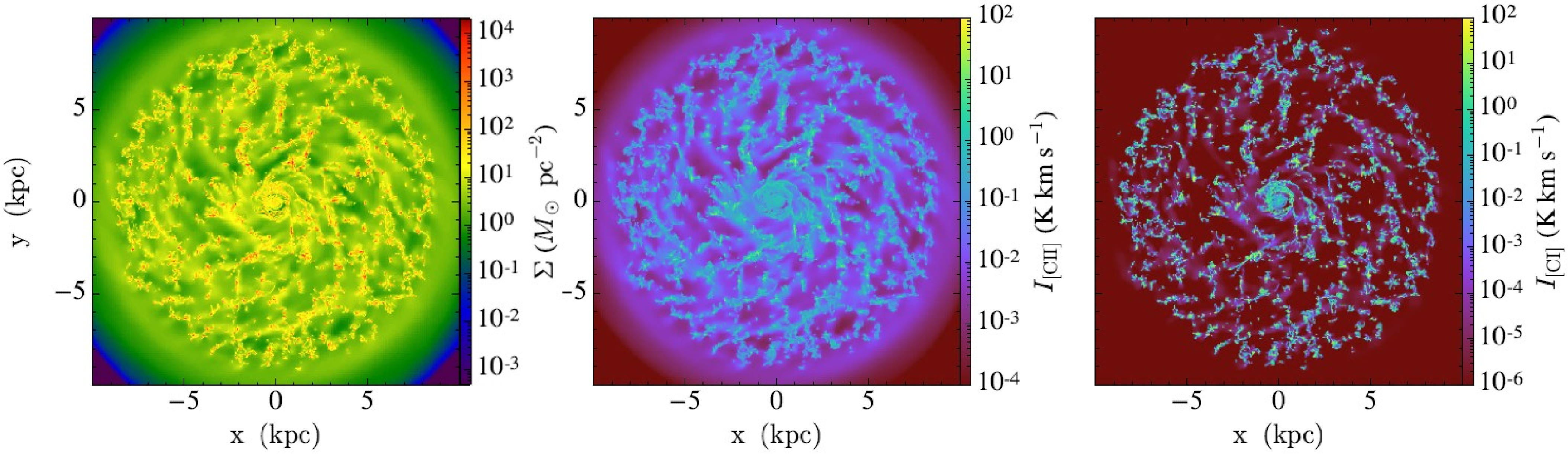

Simulations by Qi, Tan, et al., PASJ, *in press* (arXiv: 1706.03764)

Magnetohydrodynamical models

Wu et al. (2017, ApJ, 835, 137)

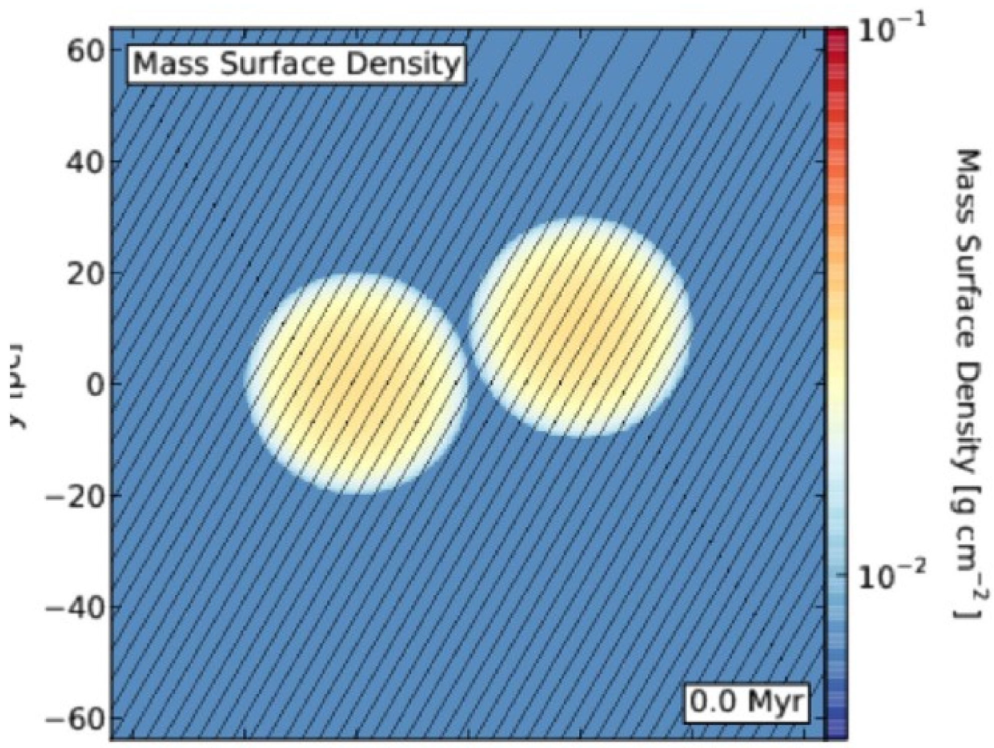

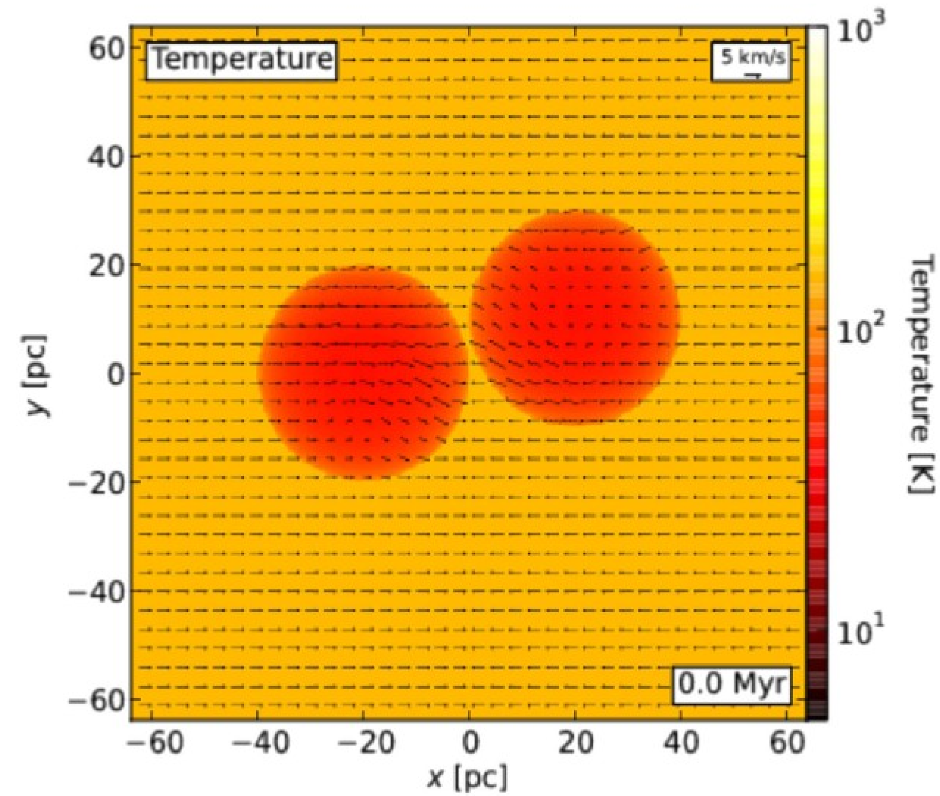

Physical processes included: self-gravity, supersonic turbulence, magnetic fields.

Initial conditions: two initially spherical GMCs of uniform density of H nuclei n_H=100 cm^{-3} and radii R_{GMC}=20pc, giving each GMC a mass M_{GMC}=9.3x10^4M_o.

The clouds are embedded in ambient gas, representing the atomic cold neutral medium, with density $n_{H,0}$=10cm^{-3}.

Magnetohydrodynamical models

Wu et al. (2017, ApJ, 835, 137)

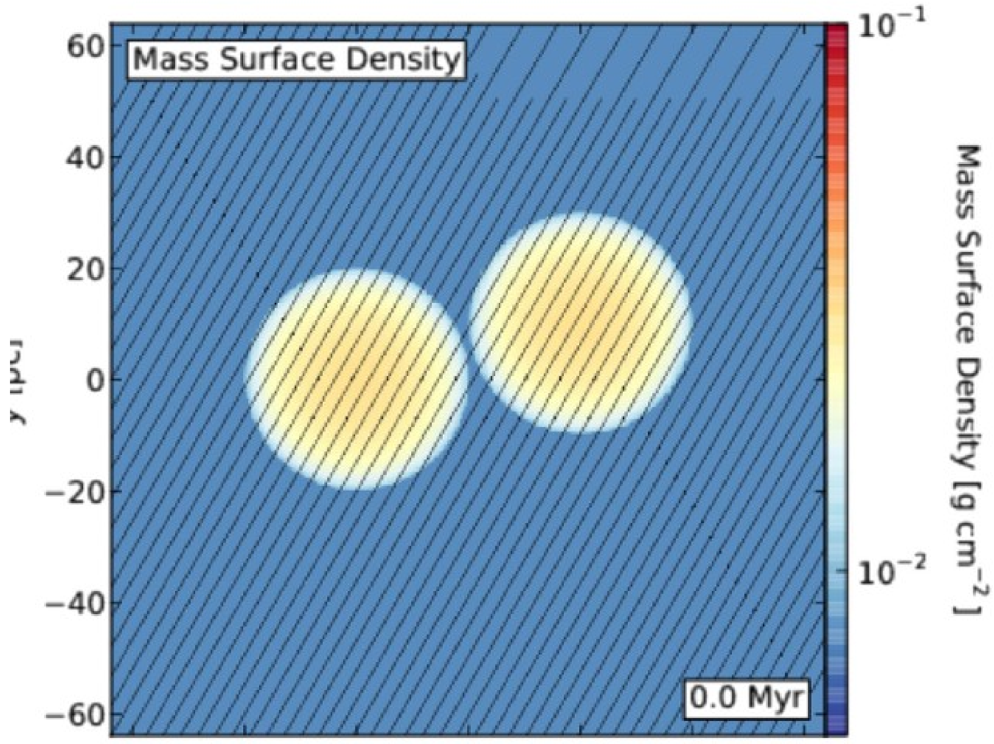

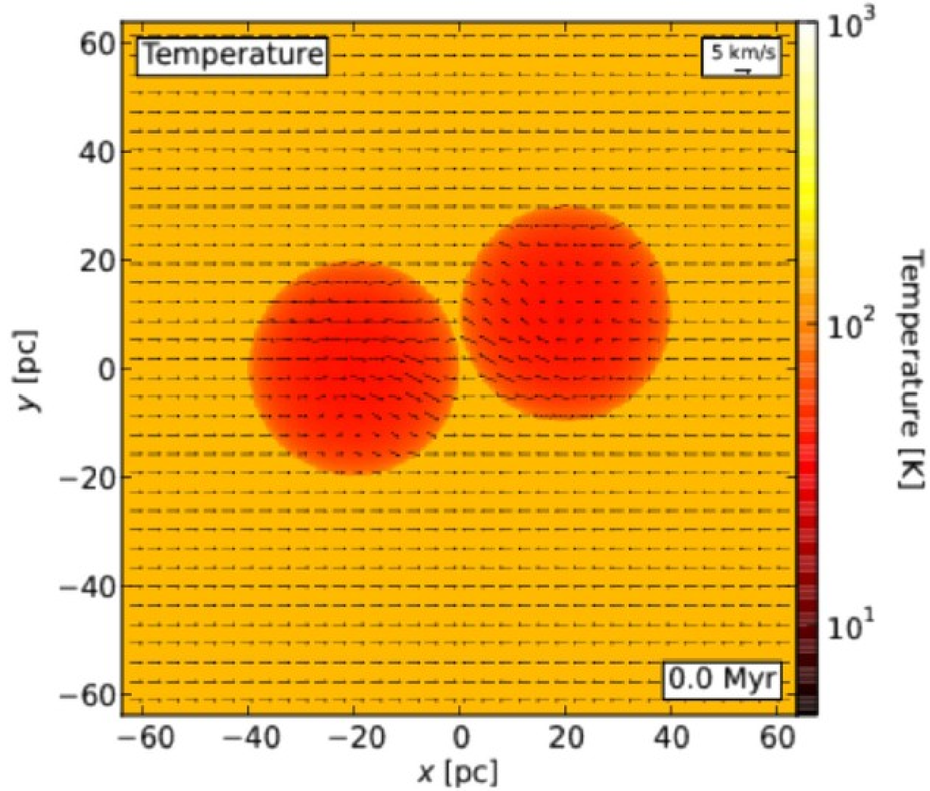

Supersonic turbulence is introduced in order to approximate the velocity and density fluctuations presented in observed GMC.

The GMCs are somewhat confined by the pressure of the ambient, uniform density medium.

The GMCs are initialized with large kinetic energies and this done to avoid rapid global collapse within the first few Myrs.

Magnetohydrodynamical models

Wu et al. (2017, ApJ, 835, 137)

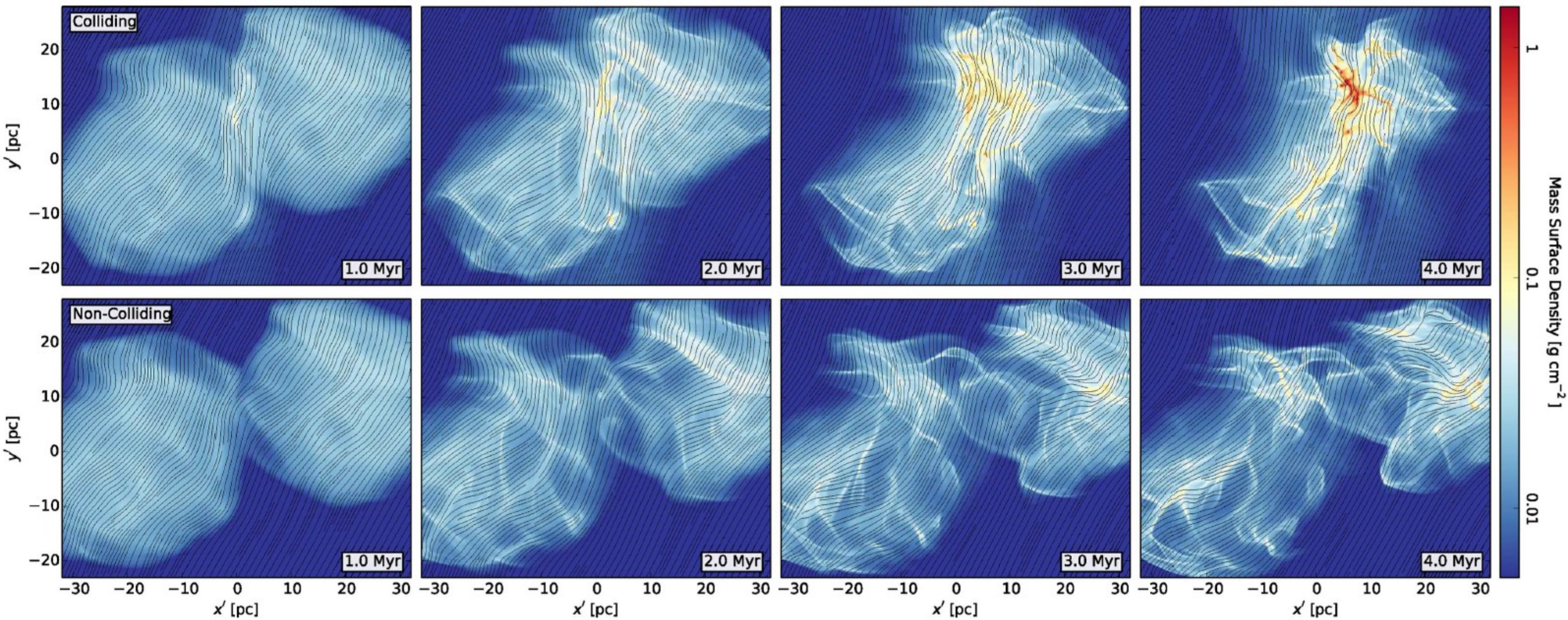

We select two different cases from the Wu et al. simulations:

a) the case where the clouds collide (upper row) at a relative speed of 10km/s (“colliding”)

b) the case where the clouds do not collide (lower row, “non-colliding”)

The collision occurs along the x-direction.

Example of a synthetic observation

(Haworth et al., 2015, MNRAS, 450, 10)

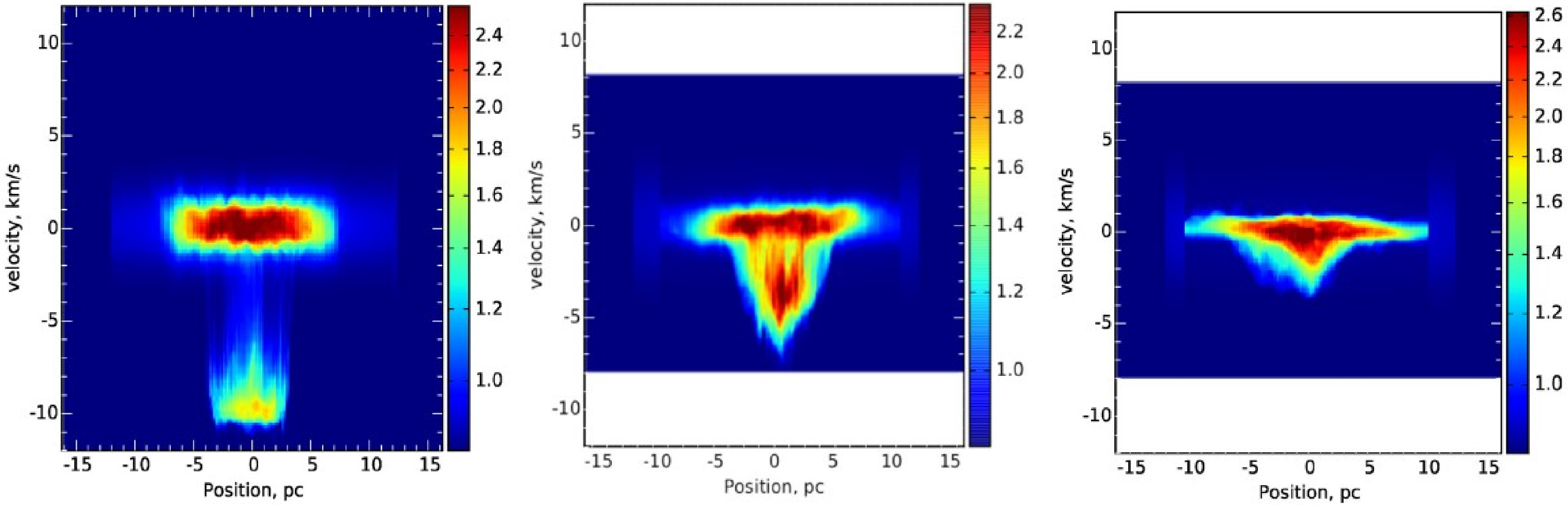

In this example, two uniform density GMCs are colliding along the line of sight.
There is no PDR chemistry included here; instead a constant CO abundance is assumed.

By including PDR calculations we are able to study how lines of other coolants behave when a GMC-GMC collision occurs, and thus whether or not new diagnostics can occur.

Synthetic observations of cloud-cloud collision: [CII] 158um as a new diagnostic

(Bisbas, Tanaka, Tan, et al., 2017, ApJ, 850, 23)

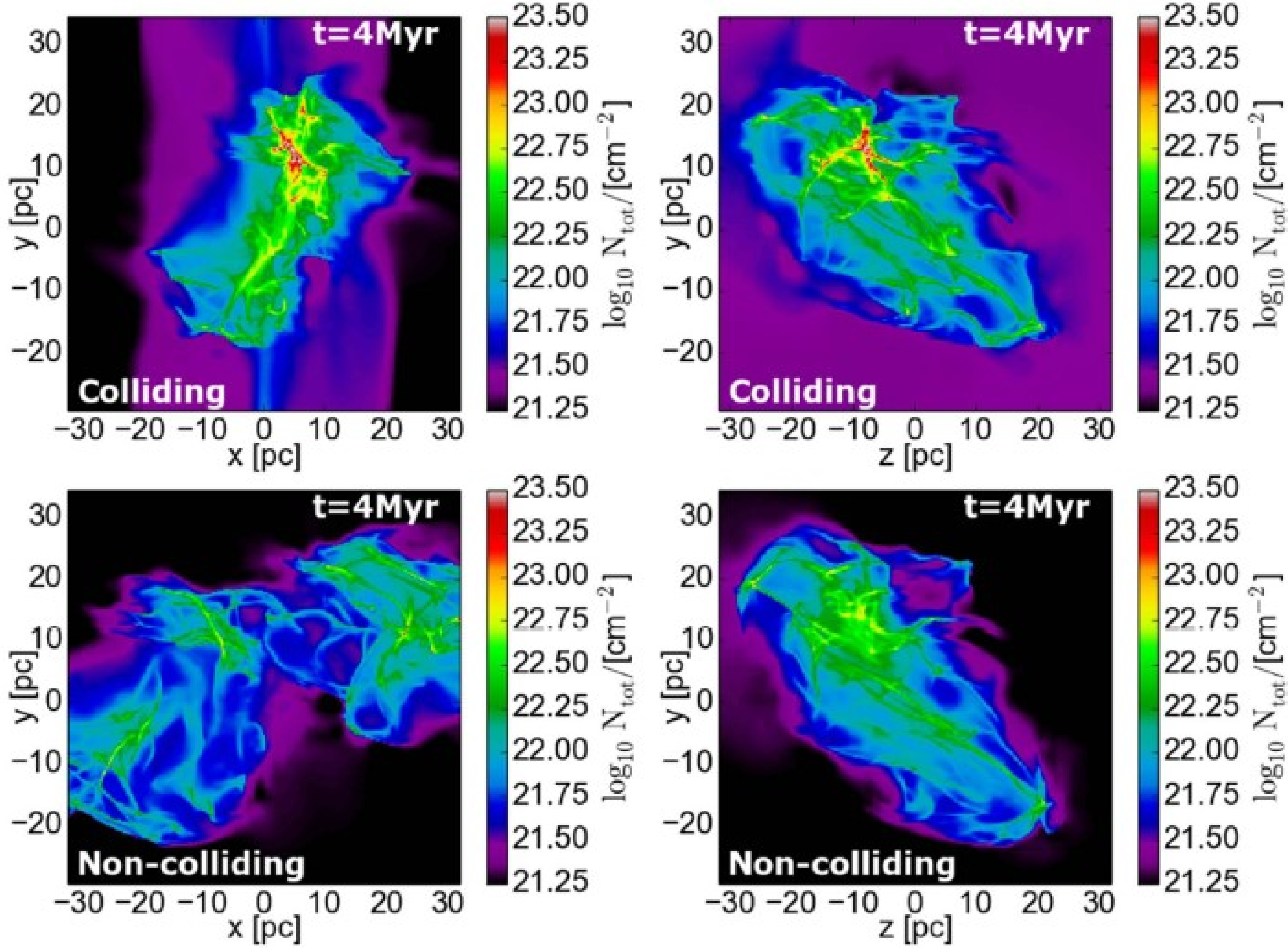

3D-PDR

3D-PDR - The first fully 3D code for PDRs

View on GitHub | Download .zip | Download .tar.gz

3D-PDR is a three-dimensional photodissociation region code written in Fortran. It uses the Sundials package (written in C) to solve the set of ordinary differential equations and it is the successor of UCL_PDR, a one-dimensional PDR code written at UCL. Using the HEALpix ray-tracing scheme, 3D-PDR solves a three-dimensional escape probability routine and evaluates the attenuation of the far-ultraviolet radiation in the PDR and the propagation of FIR/submm emission lines out of the PDR.

The code is parallelized (OpenMP) and can be applied to 1D and 3D problems. The GitHub package includes: the 3D-PDR code, three different chemical networks (33, 58, and 128 species) and molecular data, the Sundials solver, and a set of various 1D uniform density clouds and a uniform density spherical distribution to test the 3D version of the code. To `make' 3D-PDR, you will first need to install the Sundials package and link 3D-PDR with the ODE solver. Please see the manual for instructions on how to do this step-by-step.

3D-PDR works with the gfortran version 4.8.4 and the ifort version 14.0.4. Later compiler versions may require adjustments in the code.

Bisbas et al. 2012, MNRAS, 427, 2100

Download the code: **https://uclchem.github.io/3dpdr.html**

Synthetic observations of cloud-cloud collision: [CII] 158um as a new diagnostic

(Bisbas, Tanaka, Tan, et al., 2017, ApJ, 850, 23)

Snapshot at 2 Myr

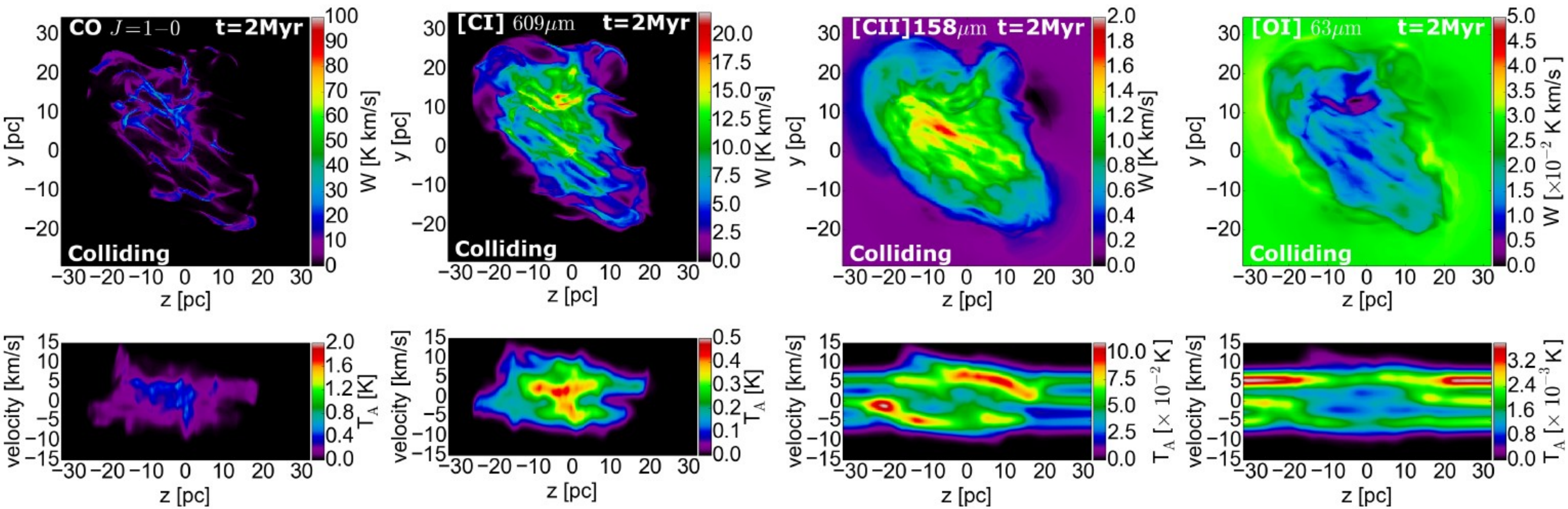

From left to right: CO(1-0), [CI] 609um, [CII] 158um, [OI] 63um.
Upper panels show the emission map (K km/s)
Lower panels show the average p-v diagram. Colours correspond to the antenna temperature (K).

Synthetic observations of cloud-cloud collision: [CII] 158um as a new diagnostic

(Bisbas, Tanaka, Tan, et al., 2017, ApJ, 850, 23)

Snapshot at 4 Myr

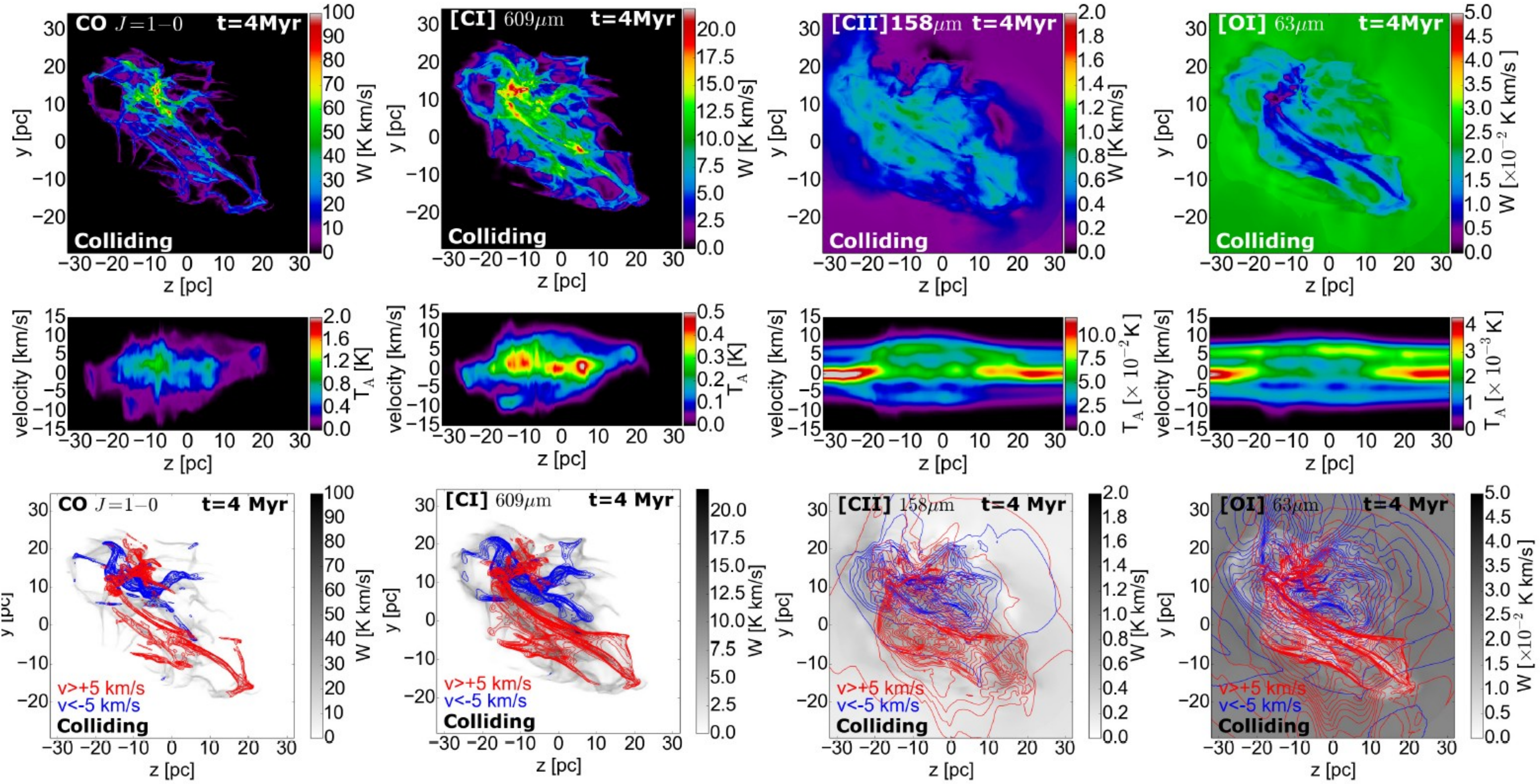

Synthetic observations of cloud-cloud collision: [CII] 158um as a new diagnostic

(Bisbas, Tanaka, Tan, et al., 2017, ApJ, 850, 23)

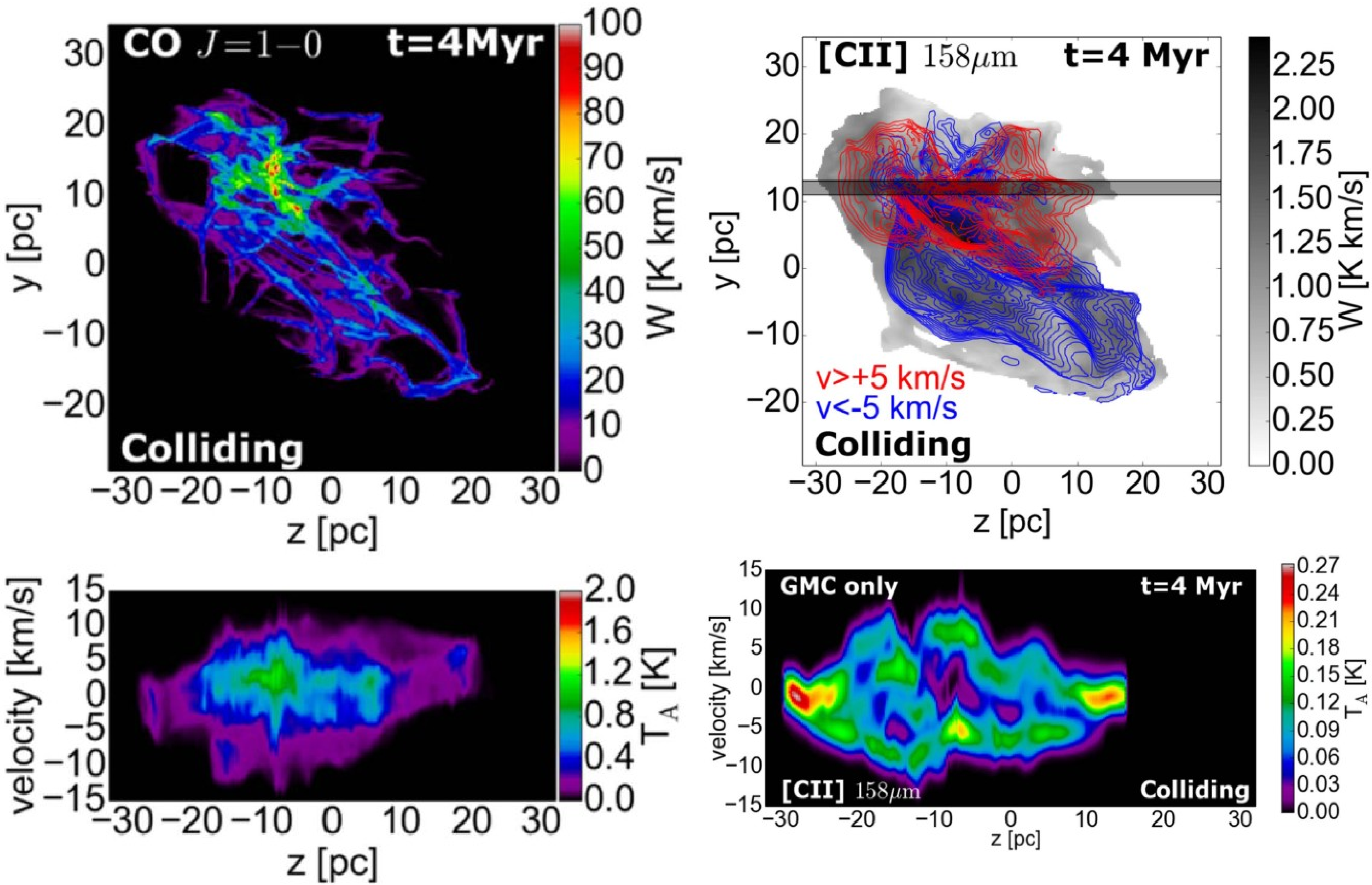

The inception of star cluster formation: new SOFIA observations (Bisbas, Tan, Csengeri et al., 2018, MNRAS Letters, *in press*)

Infrared Dark Clouds (IRDCs) are dense parts of molecular clouds, discovered due to their mid-infrared absorption of Galactic background light (Perault et al. 1996; Egan et al. 1998)

Their characteristic masses, sizes and densities, indicate that they are likely to be precursors of star-forming clumps and star clusters (e.g. Tan et al. 2014).

Since most stars form in such clusters, the study of IRDCs can reveal crucial information on the processes that set global galactic star formation rates.

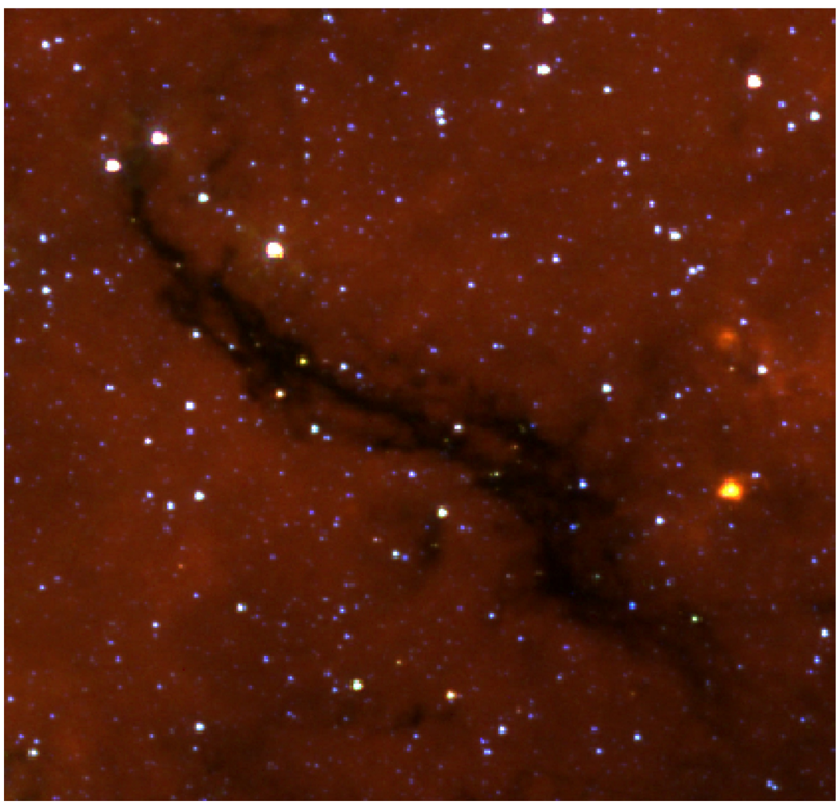

Image of the IRDC G035.39-00.33
Spitzer RGB image (R 8um, G 6um, B 3.5um)

The inception of star cluster formation: new SOFIA observations

(Bisbas, Tan, Csengeri et al., 2018, MNRAS Letters, *in press*)

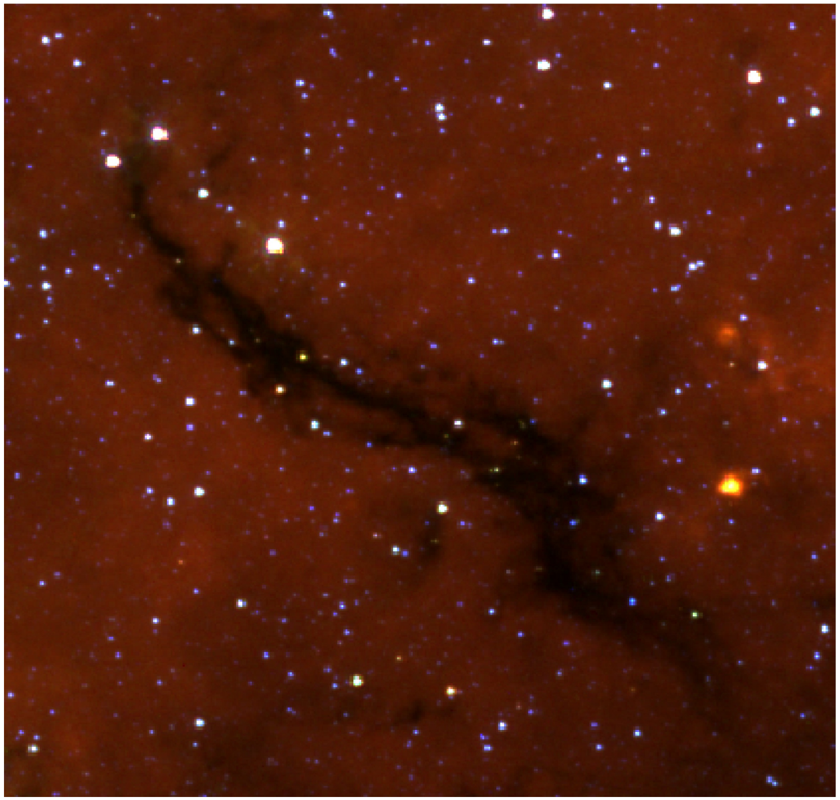

G35 is a highly filamentary cloud at a near kinematic distance of 2.9 kpc (Simon et al. 2006).

Parsec-scale SiO(2-1) emission has been detected which is potentially caused by large-scale shocks due to converging flows and/or a collision of two molecular clouds (Jimenez-Serra et al. 2010).

It has been also discovered widespread CO depletion in the dense IRDC filament (Hernandez et al. 2011), as well as constraining filament dynamics (Hernandez et al. 2012) with indications its inner regions are virialized.

We observed G35 in [CII] 158um using the SOFIA-upGREAT instrument (Risacher et al. 2016), with the primary goal of understanding the lower density atomic layers around the dense gas structure to constrain models of star formation conditions of such clouds and thus the initiation of star cluster formation.

The upGREAT receiver was on-board SOFIA on 18th May 2016 as part of the program 04_0169 (PI: Tan).

The inception of star cluster formation: new SOFIA observations

(Bisbas, Tan, Csengeri et al., 2018, MNRAS Letters, *in press*)

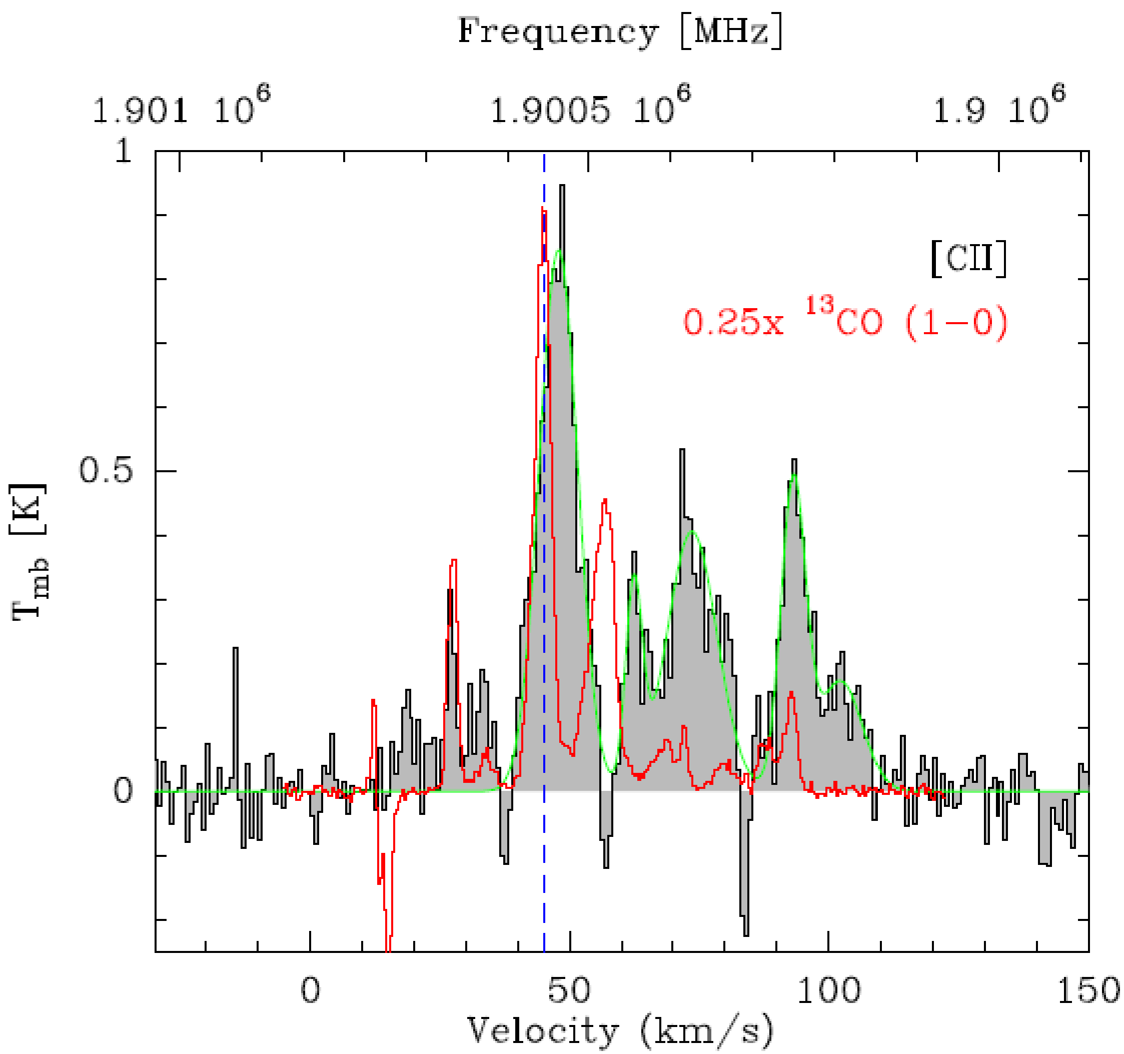

Gray filled histogram shows the [CII] spectrum averaged over the entire mapped region of G35. The GRS 13CO(1-0) spectrum (Jackson et al. 2006) averaged over the same region is shown in red.

The upper x axis shows the signal band frequency scale for the [CII] data. For better visibility, the 13CO spectrum is scaled by a factor of 0.25. The blue dashed line shows v_{lsr} of G35.

The inception of star cluster formation: new SOFIA observations (Bisbas, Tan, Csengeri et al., 2018, MNRAS Letters, *in press*)

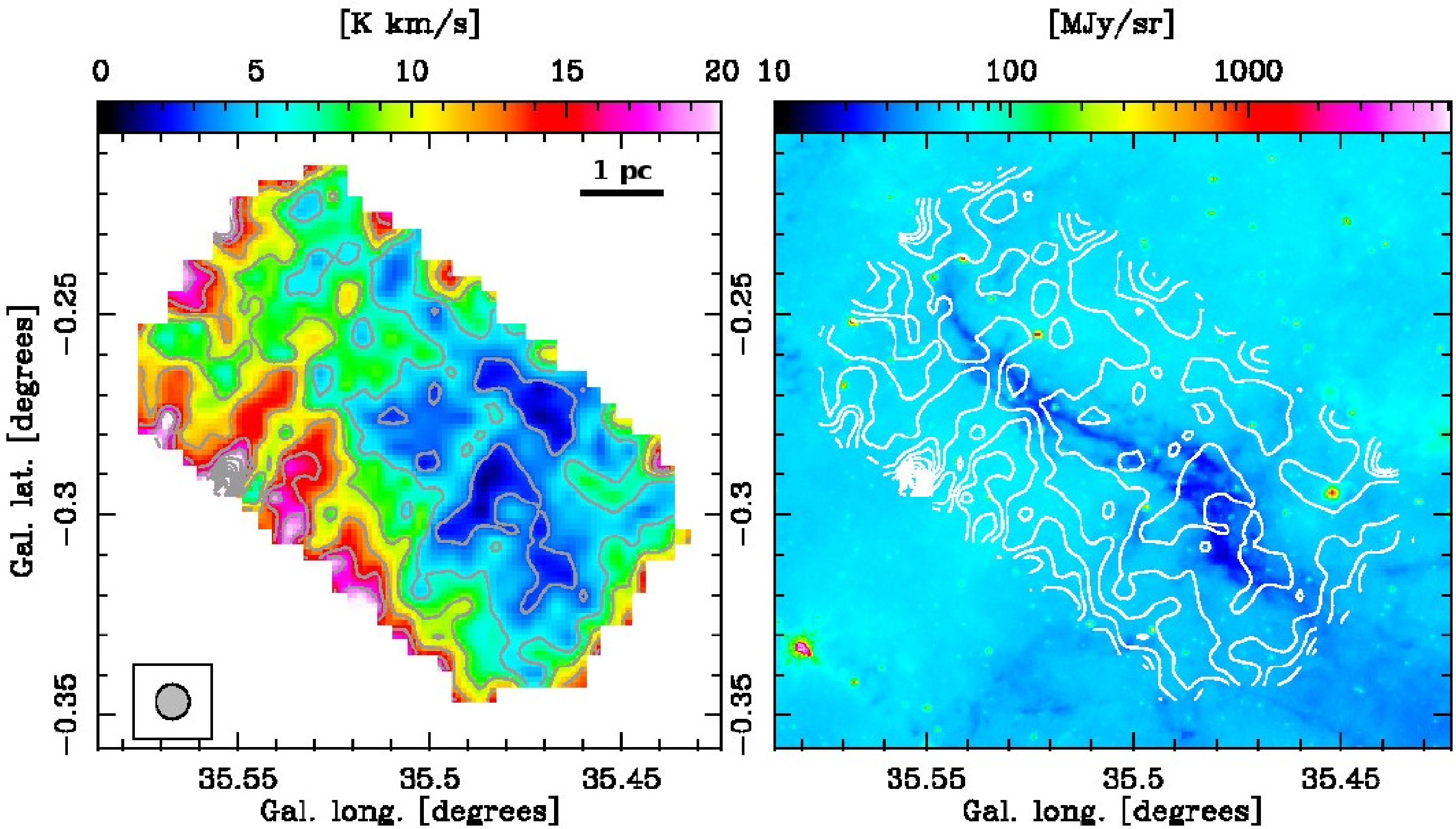

Left: Integrated emission of [CII] between 40 to 55 km/s corresponding to the brightest velocity component close to the v_{lsr} of G35. A linear scale of 1 pc for an adopted distance of 2.9 kpc is shown. *Right*: Spitzer 8 um map of the region. G35 is seen in absorption against the Galactic background.

The inception of star cluster formation: new SOFIA observations

(Bisbas, Tan, Csengeri et al., 2018, MNRAS Letters, *in press*)

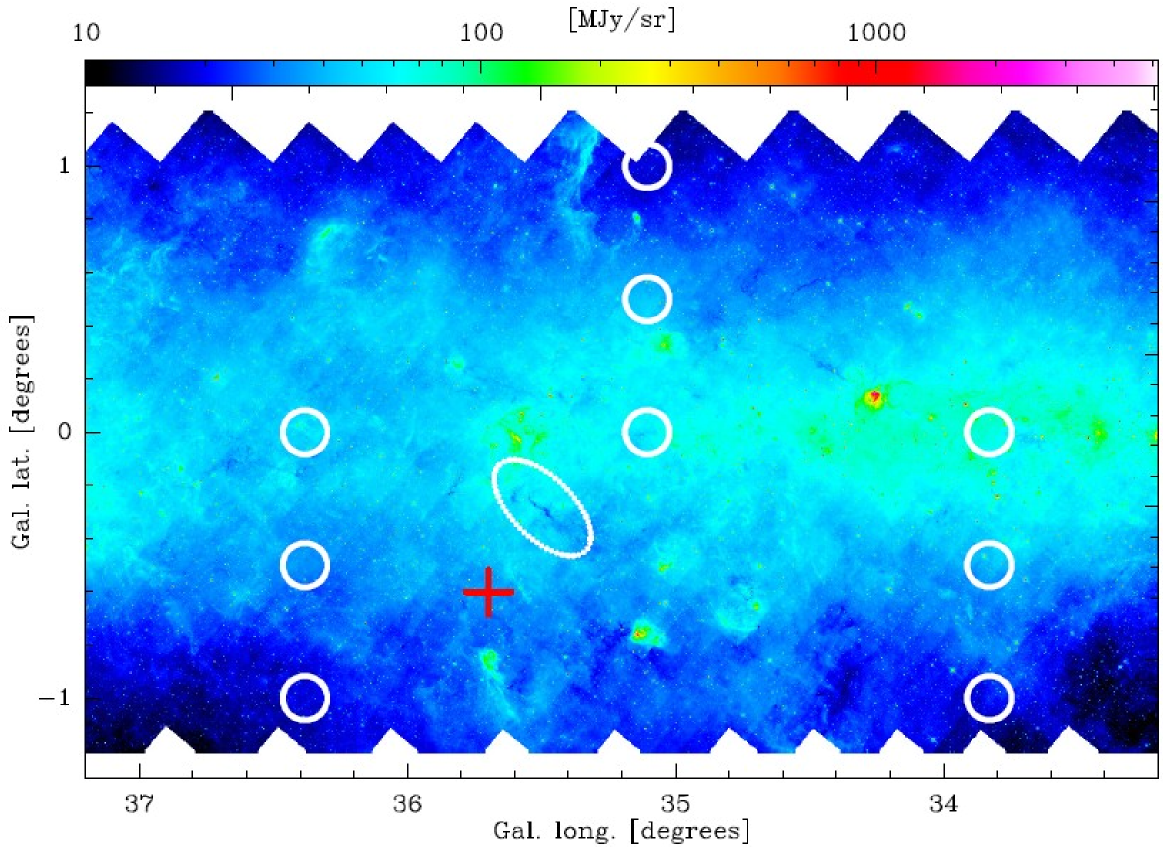

Top panel: 8um showing the area surrounding G35 in the Galactic plane. The centre of each white circles is Herschel's [CII] observations (GOT C+ Pineda et al. 2013; Langer et al. 2014). The white ellipse indicates the position of G35, which is close to the G035+0.0 GOT C+ observation. The red cross shows the OFF position of our observations. **Bottom row**: Blue, green and red solid lines correspond to the GOT C+ observations of [CII] 158 um for the 9 nearby regions to IRDC H. The solid black line in each panel shows the SOFIA [CII]data towards IRDC H.

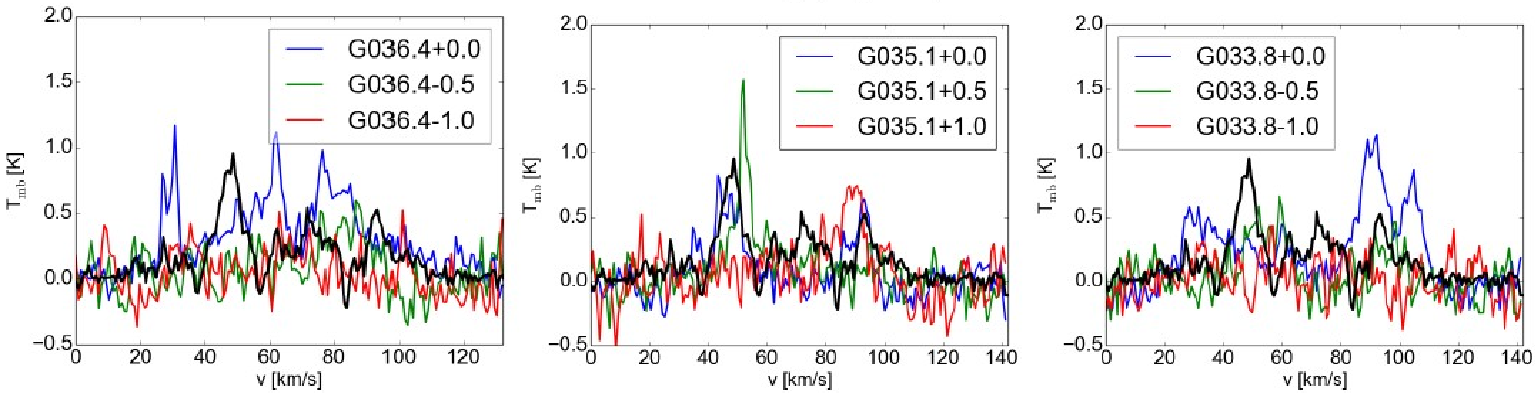

The inception of star cluster formation: new SOFIA observations

(Bisbas, Tan, Csengeri et al., 2018, MNRAS Letters, *in press*)

Observations

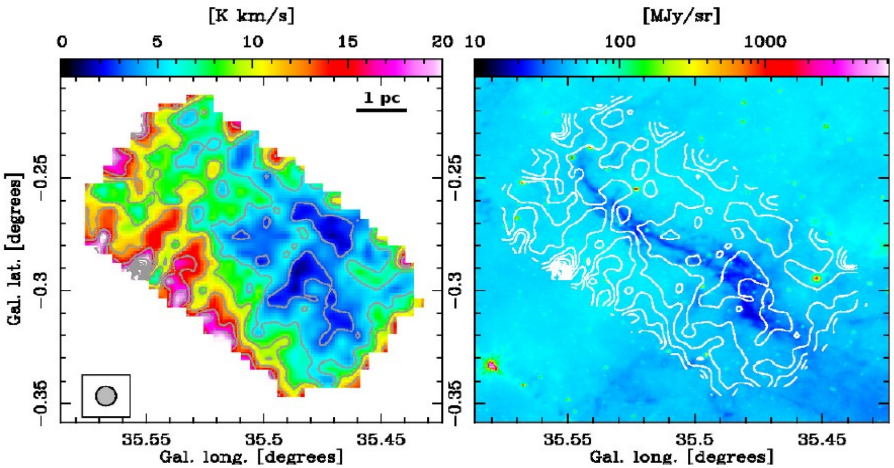

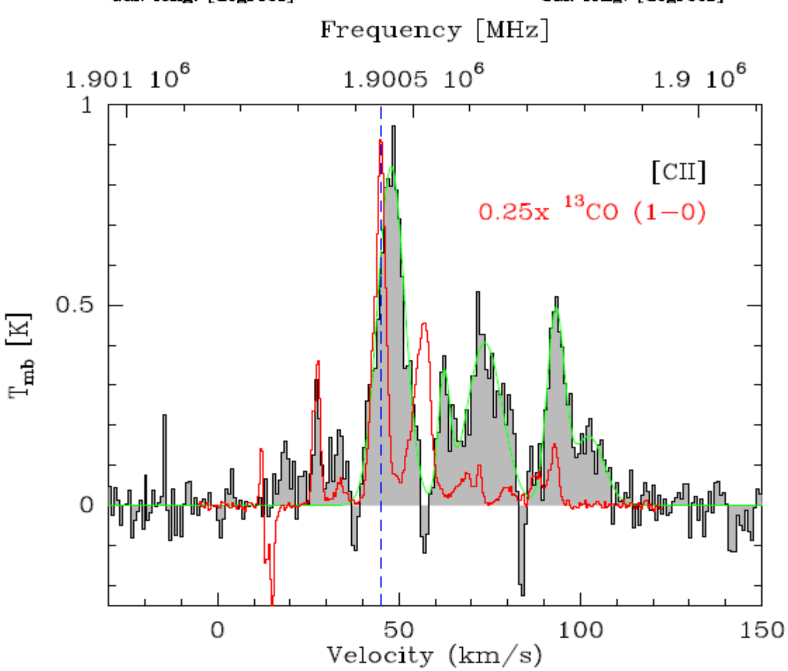

3D-PDR Simulations

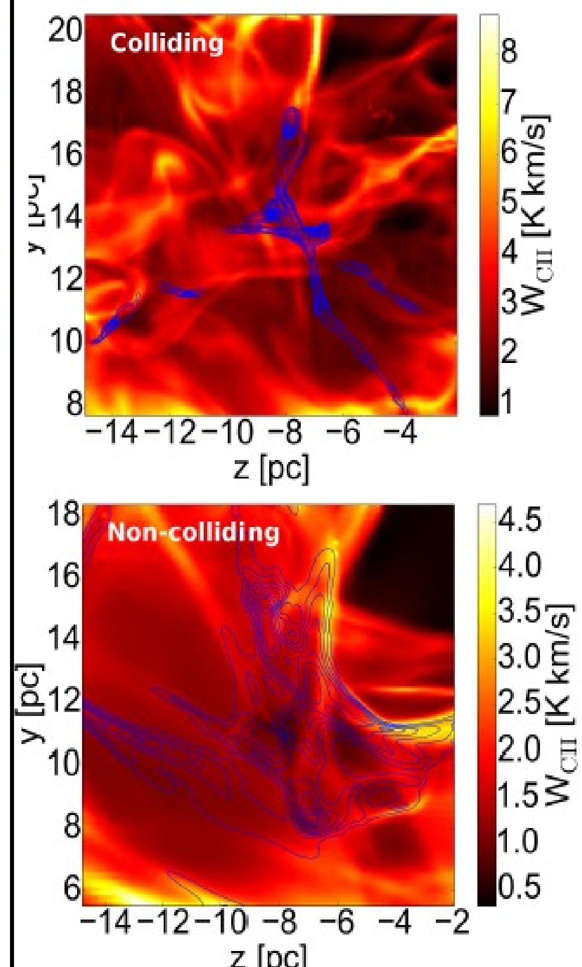

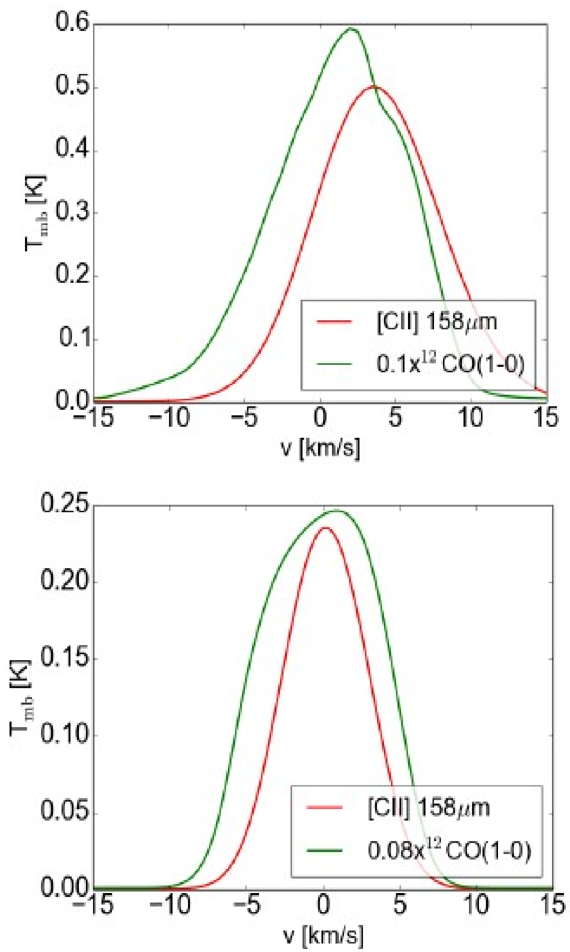

The inception of star cluster formation: new SOFIA observations

As we saw in the spectrum earlier, a primary peak of brightness temperature is observed at ~45km/s, and a secondary one at ~55km/s.

Such a difference of ~10 km/s, together with their known connection in p-v space and the observed SiO(2-1) emission, strengthens the GMC-GMC collision scenario as the most probable formation mechanism of G35.

This is the first such example of GMC collision producing dense gas that likely leads to star cluster formation

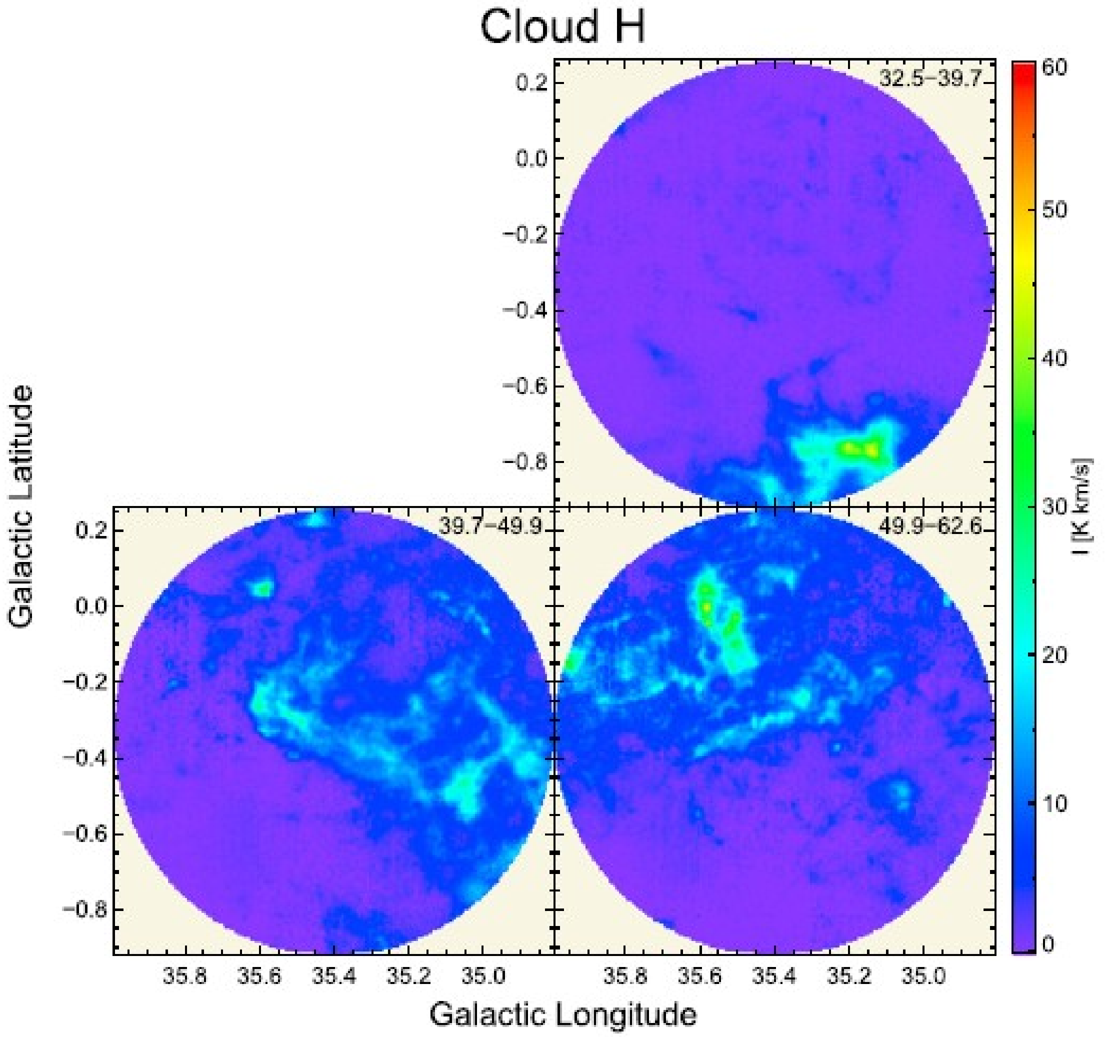

13CO(1-0) observations of G35 area by ***Hernandez et al., 2015, ApJ, 809, 154.***

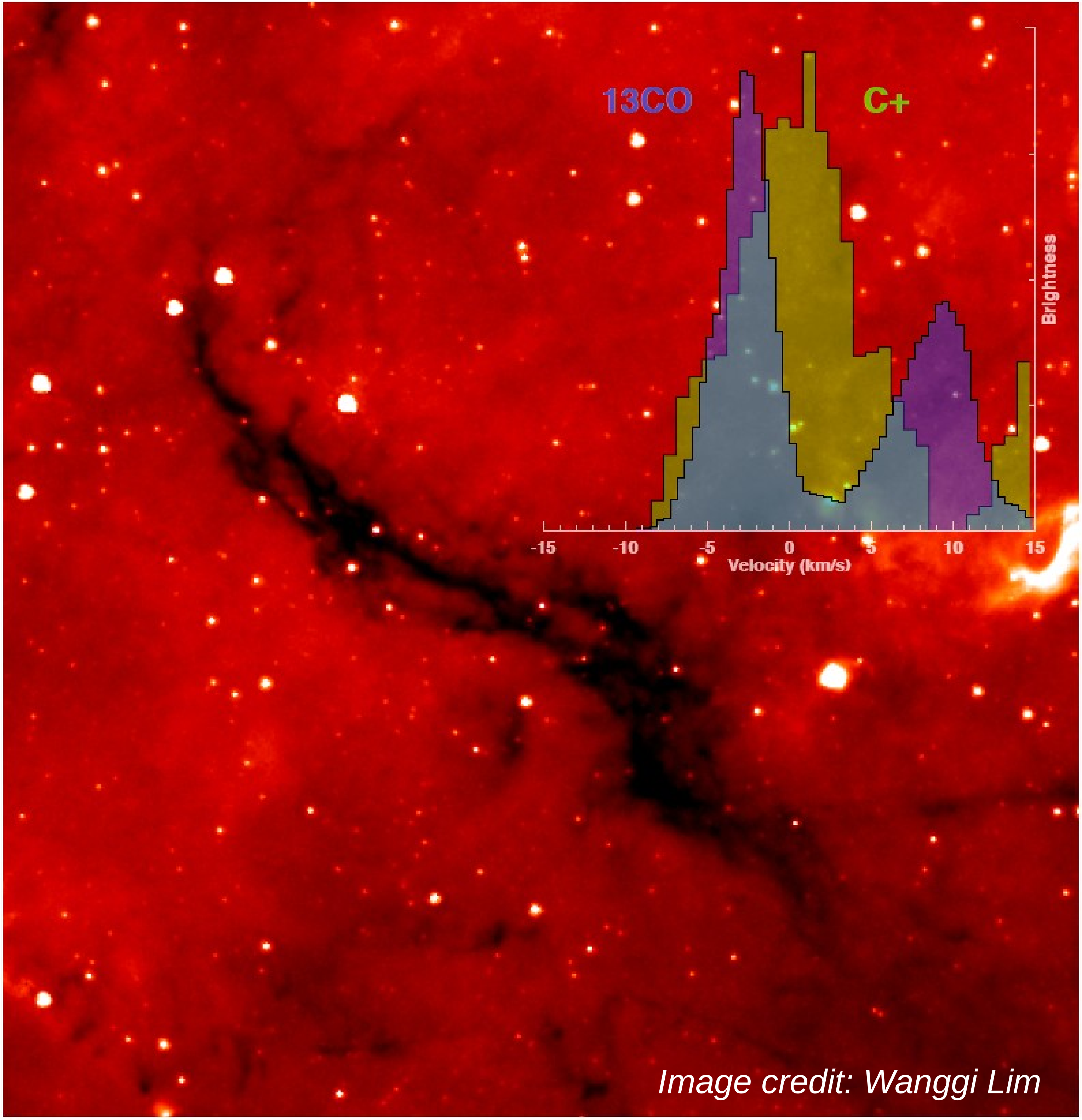
13CO
C+
Brightness
-15
-10
-5
0
5
10
15
Velocity (km/s)
Image credit: Wanggi Lim

Conclusions

1. We have presented SOFIA-upGREAT observations of [CII] 158um emission in a well-studied filamentary IRDC.

2. We find that the integrated emission of [CII] is spatially offset compared to the dense structure of the IRDC, as seen in absorption of 8um against the Galactic background.

3. We performed 3D-PDR calculations where we post-processed two snapshots of a "colliding" and "non-colliding" case of overlapping GMCs along the line of sight.

4. We find that our synthetic observations reproduce the features of the G35 observed data in the "colliding" scenario only, strengthening the evidence that this IRDC is a result of a GMC-GMC collision.

There are still alternative possibilities. For example, the [CII] emission may simply trace the turbulent boundary region of a massive GMC or GMC complex, of which G35 only represents one small part. Higher sensitivities are also needed to enable higher resolution spatial mapping of the [CII] emission. Such observations can help improve our understanding of IRDC formation and thus the processes that initiate star cluster formation and control the star formation rates of galaxies.

Thomas G. Bisbas
tbisbas@gmail.com

UNIVERSITY of VIRGINIA